Carbohydrate Polymers 332 (2024) 121844

Contents lists available at ScienceDirect

Carbohydrate Polymers

journal homepage: www.elsevier.com/locate/carbpol

The immunogenicity of p24 protein from HIV-1 virus is strongly supported and modulated by coupling with liposomes and mannan

K. Zachová [a], E. Bartheldyová [b], F. Hubatka [b], M. Křupka [a], N. Odehnalová [b], P. Turánek Knötigová [b], N. Vaškovicová [c], K. Sloupenská [a], R. Hromádka [b], E. Paulovičová [d], R. Effenberg [e], M. Ledvina [e], M. Raška [a,*], J. Turánek [a,b,f,**]

[a] Department of Immunology, Faculty of Medicine and Dentistry, Palacky University Olomouc and University Hospital Olomouc, Hněvotínská 3, Olomouc, Czech Republic
[b] C2P NEXARS, The Campus Science Park, Palachovo náměstí 2, Brno, Czech Republic
[c] Faculty of Medicine, Masaryk University, Kamenice 5, Brno, Czech Republic
[d] Center for Glycomics, Institute of Chemistry, Slovak Academy of Sciences, Dúbravská cesta 9, Bratislava, Slovakia
[e] Department of Chemistry of Natural Compounds, University of Chemistry and Technology, Technická 5, Prague, Czech Republic
[f] Institute of Clinical Immunology & Allergology, Charles University Prague and University Hospital, Hradec Kralove, Sokolská 581, Hradec Kralove, Czech Republic

ARTICLE INFO

Keywords:
Liposomes
Mannan
Recombinant protein
Adjuvants
Bioconjugation
Oxime ligation

ABSTRACT

Anti-viral and anti-tumor vaccines aim to induce cytotoxic CD8+ T cells (CTL) and antibodies. Conserved protein antigens, such as p24 from human immunodeficiency virus, represent promising component for elicitation CTLs, nevertheless with suboptimal immunogenicity, if formulated as recombinant protein. To enhance immunogenicity and CTL response, recombinant proteins may be targeted to dendritic cells (DC) for cross presentation on MHCI, where mannose receptor and/or other lectin receptors could play an important role.

Here, we constructed liposomal carrier-based vaccine composed of recombinant p24 antigen bound by metallochelating linkage onto surface of nanoliposomes with surface mannans coupled by aminooxy ligation. Generated mannosylated proteonanoliposomes were analyzed by dynamic light scattering, isothermal titration, and electron microscopy. Using murine DC line MutuDC and murine bone marrow derived DC (BMDC) we evaluated their immunogenicity and immunomodulatory activity.

We show that p24 mannosylated proteonanoliposomes activate DC for enhanced MHCI, MHCII and CD40, CD80, and CD86 surface expression both on MutuDC and BMDC. p24 mannosylated liposomes were internalized by MutuDC with p24 intracellular localization within 1 to 3 h.

The combination of metallochelating and aminooxy ligation could be used simultaneously to generate nanoliposomal adjuvanted recombinant protein-based vaccines versatile for combination of recombinant antigens relevant for antibody and CTL elicitation.

1. Background

In spite of long term intensive research and development worldwide the effective vaccine against HIV-1 is still an unattained goal. The protein p24 is a part of gag polyprotein from HIV-1 representing a relatively poor immunogen but with considerably conserved structure, which is the advantage making the viral p24 protein an appropriate candidate component in an HIV-1 prophylactic vaccine development. There is a vital need of improved adjuvants for the development of recombinant subunit vaccines. Especially adjuvants inducing also mucosal immunity are of importance for vaccines against pathogens invading the body via mucosal surfaces. The immunogenicity of proteins could be stimulated or modulated by many different ways. Basically, coupling the antigen with different immunologically active compounds affects it's internalization by antigen presenting cells (APCs), it's intracellular processing and subsequently it's presentation on the cell surface through MHC molecules (Zachova, Krupka, & Raska, 2016). The antigen internalization, as the first step in antigen presentation, was described to play an

* Corresponding author.
** Correspondence to: J. Turánek, Department of Immunology, Faculty of Medicine and Dentistry, Palacky University Olomouc, Hněvotínská 3, 779 00 Olomouc, Czech Republic.
E-mail addresses: milan.raska@upol.cz (M. Raška), turanek@seznam.cz (J. Turánek).

https://doi.org/10.1016/j.carbpol.2024.121844
Received 14 September 2023; Received in revised form 31 December 2023; Accepted 18 January 2024
Available online 23 January 2024

essential role in modern prophylactic vaccine development. Therefore, there is an intensive trend to make recognition and internalization of antigen as effective as possible. Liposomes represent important biocompatible and FDA-approved delivery systems for peptides, proteins, drugs, and other compounds. Appropriate surface modification of liposomes endowed them with ability to be targeted toward various cells and tissues within the organism. In the case of vaccines development targeting the APCs it is of great importance. For this purposes antigens could be coupled with liposomes (Arab et al., 2018; Bulbake, Doppalapudi, Kommineni, & Khan, 2017; De Serrano & Burkhart, 2017; Krupka et al., 2012; Masek et al., 2011; Masek et al., 2011), where the liposomes could be diversely modified (Bartheldyova et al., 2019; Cawlfield et al., 2019; Petrokova et al., 2019; Qu et al., 2018). Also nanodiscs (Kuai et al., 2018) or heat shock proteins (Krupka et al., 2015; Martin et al., 2003; Stocki, Wang, & Dickinson, 2012; Vo et al., 2017; Zachova et al., 2016) represent possible systems for coupling of antigens to improve their internalization by APCs. Post-modifications of liposomes may influence the antigen cross presentation by APCs. Immunogenicity of liposome-coupled antigens is also influenced by size of vesicle, surface charge, composition of bilayer, lamellarity, and co-encapsulation with molecular adjuvants. (Bartheldyova et al., 2019; Effenberg et al., 2017; Knotigova et al., 2015; Krupka et al., 2016; Nagy et al., 2022; Nam et al., 2022).

Since 2011, when we have published our first paper on binding of HisTag recombinant protein onto liposomal surface via metallochelating bond, we belong to teams pioneering research in application of proteoliposomes for development of vaccines and theranostics (Effenberg et al., 2017; Knotigova et al., 2015; Koudelka et al., 2016; Krupka et al., 2016).

In present study we have combined a two formerly described methods to generate mannosylated liposomes coupled with p24 antigen (Bartheldyova et al., 2019; Krupka et al., 2012; Masek, Bartheldyova, Turanek-Knotigova, et al., 2011). The mannan molecules isolated from *C. glabrata* were coupled onto liposomal surface by orthogonal reaction based on a click chemistry (aminooxy coupling) (Bartheldyova et al., 2019). This method yielded perfect orientation of all mannan molecules similarly to the structures on the cell wall of *C. glabrata*. Therefore, liposomes modified by mannan can be effectively recognized and internalized by dendritic cells via receptors recognizing mannose-containing structures such as mannose receptor (MR). Moreover, mannans represent a dangerous signal and could act as molecular adjuvants inducing also mucosal immune response.

This study is focused on preparation of vaccination nanoparticles based on nanoliposomes with surface-bound mannan and recombinant p24 protein bound onto nanoliposomes surface via metallochelating binding. Immunological properties of p24 protein (p24), p24 protein coupled with liposome (p24L) and p24 protein coupled with mannosylated liposome (p24LM) was tested on two in vitro models of murine dendritic cells. The first model was based on the bone-marrow derived dendritic cells from BALB/c mice representing the H2kD haplotype and the second one was MutuDC-immortalized cell line from splenocytes of C57BL/6 mouse representing the H2kB haplotype.

Our study demonstrates potential application of this type of liposomal vaccination nanoparticles for development of novel vaccines. Complex immune response further supplemented with virus surface proteins-specific antibodies is required in the case of HIV-1 and other viruses infection.

2. Results

2.1. Preparation of liposomes

Metallochelating liposomes containing DGS-NTA-Ni and N-oxy lipid were prepared by lipid hydration method followed by extrusion through 100 nm filter. His-tagged p24 antigen and mannan molecules were bounded consequently to the liposomal surface via metallochelation and oxime ligation as shown in Fig. 1A, respectively. The binding of particular components was reflected by an increase in the hydrodynamic radius of all, p24 proteoliposomes (p24L - 103 nm), mannosylated liposomes (LM - 119 nm) and p24 mannosylated liposomes (p24LM 121 nm) as compared to the hydrodynamic radius of plain liposomes (94 nm) (Fig. 1B). The increase in the size corresponds well to measured hydrodynamic radius of p24 protein (5.6 nm) and mannan molecule (7.1 nm).

The surface modification of liposomes with p24 antigen and mannan molecules was confirmed by immunogold staining as shown schematically in Fig. 2A, and by isothermal titration method (Fig. 2B, C). The specific staining of p24 on the surface of liposomes using anti-V5 antibody is shown in the Fig. 2DE and the presence of mannan molecules on the surface of mannosylated liposomes is shown in Fig. 2F. The recombinant mannose receptor used for specific immunogold detection confirms the functional interaction between mannose receptor and mannosylated liposomes. To prove dual modification of liposomes using p24 antigen and mannan, the modification of liposomes using mannan was done first followed by metallochelation interaction of surface exposed NTA-Ni with His-tagged p24 (Fig. 2DEF).

The stoichiometry of the reaction between Ni-ions and HisTag epitopes on the surface of liposomes and mannosylated liposomes was defined by isothermal titration calorimetry (Fig. 2, inserted table). The dissociation constant of both formulations was determined and similar values for both formulations were obtained. These results indicate no effect on the stability of the bond between liposomes and p24 antigen. Some steric hindrance of the liposome surface by mannan molecules in the case of mannosylated liposomes influences the stoichiometry of the reaction between Ni-ions and His-tagged p24 molecules (the value of 2 for metallochelation liposomes vs. 14 for mannosylated liposomes). This is in good accordance with theoretical assumption. Considering that nearly half of the Ni-ions are present in the inner layer of phospholipid bilayer, it means that almost all NTA-Ni groups present onto the liposome surface are saturated with the p24 protein.

2.2. MutuDC cells response to p24 coupled to nanoliposome and mannan

MutuDC cells were described to be a very efficient antigen presenting cell line (Fuertes Marraco et al., 2012). These cells were also characterized for their high cross-presentation activity. Therefore, markers typical for MHCII and MHCI processing such as CD40, CD80 and CD86 were characterized in detail in response to p24, p24L, p24LM (Fig. 3). Because of the cell lineage characteristics, it could be supposed that all cells react in very similar manner. This means that all activation and differentiation markers expression will be analyzed by Mean fluorescence intensity (MFI) shift among individual p24 formulation and negative control (NP).

From the analysis Fig. 3A of MutuDC being activated by three different constructs, it could be summarized that all three p24 formulations (p24, p24L and p24LM) strongly and significantly elevate the MHCI expression on the cell surface in comparison with not pulsed MutuDCs cells. On the other hand, the expression of MHCII molecules differs significantly after pulsing the cells with individual p24 formulations. The p24 protein significantly influences the MHCII expression only when bound on liposomes (p24L) or mannosylated liposomes (p24LM) in contrast to soluble p24 protein. Moreover, the p24L construct significantly increased the MHCII expression on cells in comparison to not pulsed cells.

Furthermore, significant changes in the expression of activation markers CD40, CD80, and CD86 were also detected. The p24 and p24L formulations significantly increased the CD40 marker in contrast to cells that were not pulsed. The expression of CD80 activation marker was significantly increased in all p24 formulations (Fig. 3A, C). Moreover, there was a significant difference between p24 alone and p24LM formulations. Concerning the CD86 activation marker expression it could be summarized that all three formulations increase the expression of

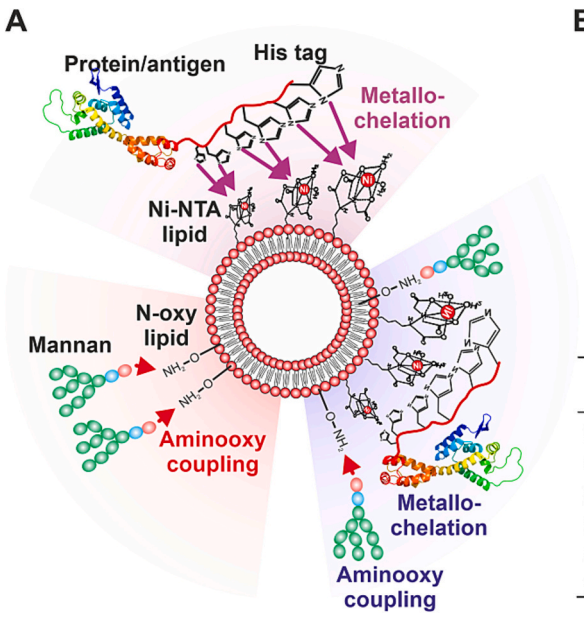

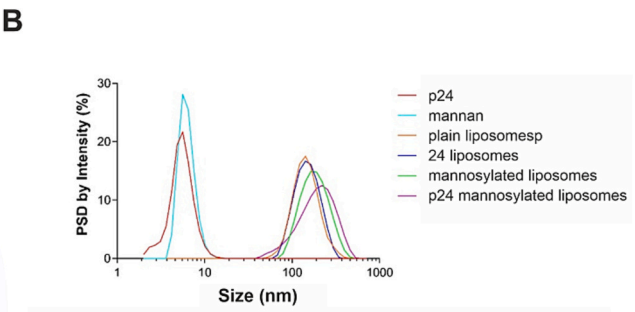

Sample	Size (nm)	PDI	Zetapotential (mV)
p24	5.6 ± 0.3	0.67 ± 0.0.2	-10.7 ± 1.6
mannan	7.1 ± 0.2	0.74 ± 0.06	-13.1 ± 1.9
plain liposomes	94.8 ± 0.2	0.09 ± 0.02	-5.4 ± 0.4
p24 liposomes	103.1 ± 2.4	0.13 ± 0.01	-6.1 ± 0.8
mannosylated liposomes	119.2 ± 0.6	0.24 ± 0.03	-6.8 ± 0.9
p24 mannosylated liposomes	121.2 ± 0.9	0.29 ± 0.01	-8.8 ± 1.5

Fig. 1. The schematic presentation of preparation and structure of liposomes modified with mannan and p24 protein and size distribution of various constructs. A) The scheme of liposome with surface orthogonally bound p24 protein via metallochelation bond and mannan molecules using click chemistry. B) The size distribution of p24, mannan molecules, and liposomes. Inserted table shows values of size based on the intensity of particles.

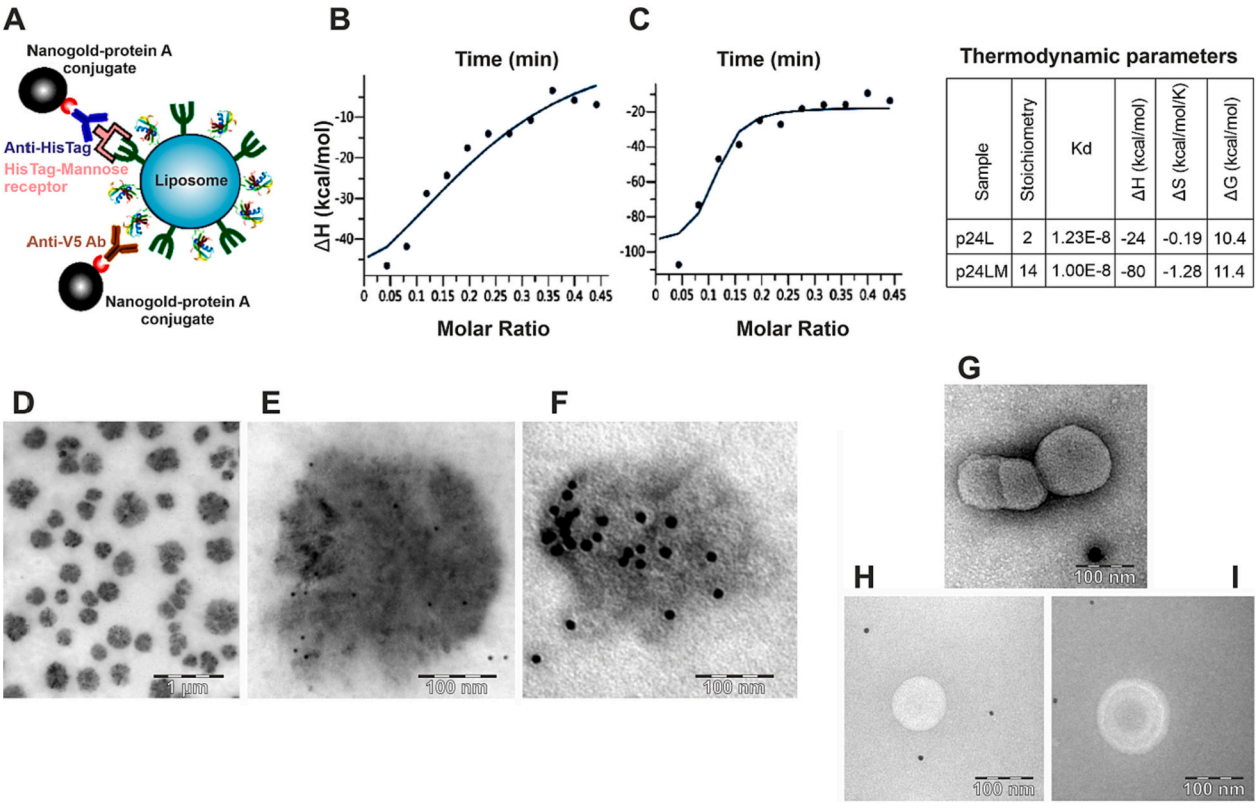

Sample	Stoichiometry	Kd	ΔH (kcal/mol)	ΔS (kcal/mol/K)	ΔG (kcal/mol)
p24L	2	1.23E-8	-24	-0.19	10.4
p24LM	14	1.00E-8	-80	-1.28	11.4

Fig. 2. Interaction of p24 protein and mannan with liposomes.
A) The scheme of the specific immunogold staining of p24 and mannan molecules. Anti-V5 antibody was used for detection of p24 antigen, whereas His-tagged recombinant mannose receptor and anti-HisTag antibody were used for the detection of mannan molecules on the surface of liposomes. B) Analysis of p24 binding on metallochelating liposomes, or C) p24 binding on mannosylated liposomes using isothermal titration. In the negative controls experiments, where no reaction enthalpy is observed, the results are shown as non-binding. Thermodynamic parameters of interaction between p24 antigen and metallochelation liposomes or mannosylated liposomes are shown in the inserted table. D) Overview image of p24 protein on the surface of liposomes visualized by anti-V5 antibody detected by protein A gold-nanoparticles. E) Detail of single liposome with immunogold stained surface p24 protein. F) p24 mannosylated liposome stained with MMR (His tagged recombinant human mannose receptor CD206) – anti-HisTag antibody – Protein A gold nanoparticles. G) Control non-stained p24 mannosylated liposomes. H) Control - p24 mannosylated liposome stained with Protein A gold nanoparticles, without MMR – HisTag antibody. I) Control - p24 mannosylated liposome stained with MMR – Protein A gold nanoparticles, without HisTag antibody.

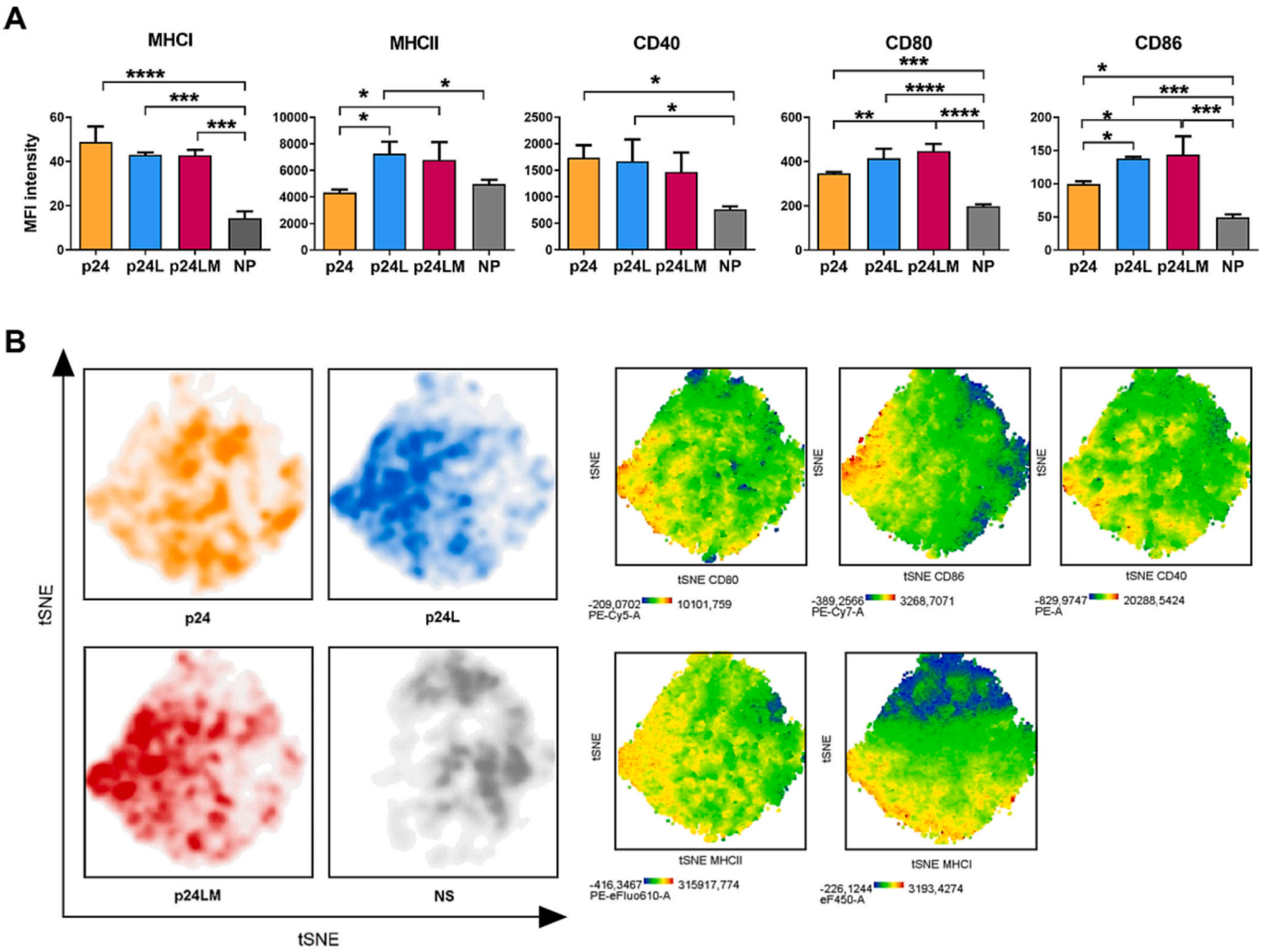

(caption on next page)

Fig. 3. MutuDC activation.
Activation of MutuDC cells by different proteo-liposomal constructs – p24 protein (p24, orange), p24 bound to liposome (p24L, blue), p24 protein bound to mannosylated liposome (p24LM, red) and not-pulsed cells (NP, grey). A) Differences of Mean fluorescence intensity corresponding to surface activation markers MHCI, MHCII, CD40, CD80, and CD86 expression on DCs pulsed by individual p24-formulations. Significance values were calculated by the ANOVA and Tukey post hoc test, where $*p < 0.05$, $**p < 0.01$, $***p < 0.001$, and $**** p < 0.0001$. B) On the left panel, the tSNE graphs of all p24-liposomal constructs showing differences in markers expression using color density are depicted. The color density of each construct is based on intensities of specific marker expressions that are shown right by HeatMap concept (FlowJo). Each HeatMap shows that the higher marker expression the more intensive shift to the left. C) CD80 surface marker expression intensity in individually pulsed samples (all pulsing experiments were performed in triplicates) using concatenation of all samples (FlowJo) and viewed by sample ID scheme. D) Constitutively GFP expressing MutuDCs (green) were pulsed by p24 bound to Liss Rhod PE labeled - mannosylated liposome (p24LM, red), stained for the cell nuclei (blue) and analyzed by confocal microscopy.

CD86 significantly comparing to negative control. Also significant differences have been determined between p24 versus p24L and p24 versus p24LM (Fig. 3A). The differences of Mean fluorescence intensity of surface marker CD86 expression are shown in Suppl. Fig. 1. These results indicate that coupling of p24 with liposomes or with mannosylated liposomes significantly increases the expression of activation marker CD86.

Summarized data of MHCI, MHCII, CD40, CD80, and CD86 expression on MutuDC are shown in tSNE projection (Fig. 3B). From this analysis it could be concluded, that the cells that were not pulsed, do not express activation markers intensively at all concerning to HeatMap projections of each marker surface expression shown on the left panel of Fig. 3B. These maps generally show that the more left the higher the marker expression intensity is. That means that the cells activated by the p24 protein express activation markers very slightly in contrast to cells activated by p24L and/or p24LM, where the intensity of all measured activation markers was markedly shifted to the left to high expression area according to particular HeatMaps.

Further, the MutuDC uptake of p24 protein coupled to mannosylated liposome (p24LM) labeled by Liss Rhod PE was analyzed by confocal microscopy (Fig. 3D). Big advantage of Liss Rhod PE labeling is in direct incorporation of fluorophore-labeled lipid into the liposomal particle and so getting specific fluorescence signal of the liposome with no background. MutuDC is a cell line that constitutively expresses GFP (green) showing the real shape of individual cell. 1 h after pulsing, p24 from p24LM formulation was located extranuclearly, close to the cell membrane of MutuDC cells.

2.3. BMDC cells response to p24 coupled to nanoliposome and mannan

Bone marrow-derived dendritic cells (BMDC) represent a group of cells differentiated from monocytes, where not all of the cells react equally. It is a heterologous cells population from which subpopulation characterized by high CD11c was selected for further analyses as the most effective cross-presenting subset (Fig. 4).

The population of cells with high expression of CD80 marker was significantly increased in BMDCs pulsed by p24 coupled to liposomes and p24 coupled to mannosylated liposomes comparing to cells that were not pulsed by any antigen or cell pulsed by p24. Simultaneously, the population with high expression of CD86 was statistically increased in case of p24 coupled to mannosylated liposomes comparing to cells pulsed by p24, p24L or cells that were not pulsed (Fig. 4A).

Concerning the MHCI and MHCII molecules cell surface expression, no significant results were determined due to big variations between the samples (Fig. 4A) nevertheless the increasing trend is obvious in all used constructs.

The tSNE projection shows that all proteo-liposomal constructs (p24, p24L, p24LM) are able to activate a cell population expressing high level of MHCI, MHCII, CD80 and CD86 markers. This population appears in the lower-left quadrant of each graph in contrast to NS group, where no such population is detectable (Fig. 4B). The intensity of marker expression is depicted by HeatMap projection representing more intensively expressed marker into left lower quadrant, as shown in Fig. 4B on the right.

In contrast to MutuDC cell line, it is possible to distinguish two separate populations characterized by low and high level of CD80 and CD86 activation marker surface expression (Fig. 4C), which indicates that after p24 stimulation specific BMDC subset emerged, characterized by $CD80^{high}$ and $CD86^{high}$. The ability to stimulate the $CD80^{high}$ population varies among p24 formulations.

Comparison of the responses to individual p24 formulations in BMDCs and MutuDC indicates similar patterns of responses concerning to the mean intensity of surface expression of CD80, CD86, MHCI, and MHCII (Table 1). Nevertheless, the activation of BMDCs (CD11c) by p24 formulations shows a dichotomy in the CD80, CD86 surface expression in stimulated BMDC cells.

From Table 1 it could be summarized that the ability to stimulate the CD80, CD86, and MHCI and MHCII expression varies among individual p24 formulations. The highest surface expression of CD80 was detected in BMDCs pulsed by p24 coupled to mannosylated liposomes followed by p24 coupled to liposomes and p24 alone. In MutuDC all characterized constructs enhanced the CD80 expression significantly. The expression of CD86 was increased after stimulation with p24 coupled to liposomes in MutuDC and mannosylated liposomes in both tested cells, but in the case of p24 alone, only MutuDC enhanced the CD86 expression significantly. In the case of MHCI, significant increase in surface expression was detected after p24 or p24 coupled to liposomes or mannosylated liposomes in comparison to not stimulated cells in MutuDC. The increase in MHCI expression was not significant in the case of BMDC, apparently due to higher variability of the responses, although the mean expression was higher. In the case of MHCII molecule, increased expression was detected after pulsing the cells with p24 coupled to liposome and mannosylated liposome, but statistically significance was detected only in MutuDC after pulsing with p24 coupled to liposomes (p24L).

2.4. Confocal microscopy

Using the antibodies specific for early endosome (anti-EEA-1) and p24-fused V5 epitope (anti-V5 – FITC), the intracellular localization of p24 was determined 1, 2, 3, and 4 h after MutuDC cells exposure to individual p24 formulations. Results are shown in Fig. 5. After pulsing the cells with p24 alone, the p24 was not detected within MutuDC for any incubation periods. In contrast, when the cells were pulsed with p24 proteoliposomes (p24L) or with p24 mannosylated proteoliposomes (p24LM) the p24 was easily detectable within the cells 1, 2 and 3 h after the pulsing, followed by antibody signal disappearance (see 4 h subpanel), indicating advanced p24 processing. To support this observation, the early endosome marker EEA1 was analyzed and it does partially co-localize with p24 at 2 and 3 h post pulsing with p24LM and even earlier when pulsed with p24L, indicating that the liposome p24 or mannosylated liposome p24 formulation supports the antigen entrapment by MutuDC using partially endosomal and partially non-endosomal clathrin-independent internalization pathway, as reported for liposomes earlier (Alshehri, Grabowska, & Stolnik, 2018; Kanamala, Palmer, Ghandehari, Wilson, & Wu, 2018; Rayamajhi et al., 2020). Partial p24 co-localization with early endosome may be due to accelerated proteoliposome processing leading to rapid shift of the antigen to the late endosome (Shearer & Petersen, 2019). Nevertheless this needs to be experimentally addressed in future experiments.

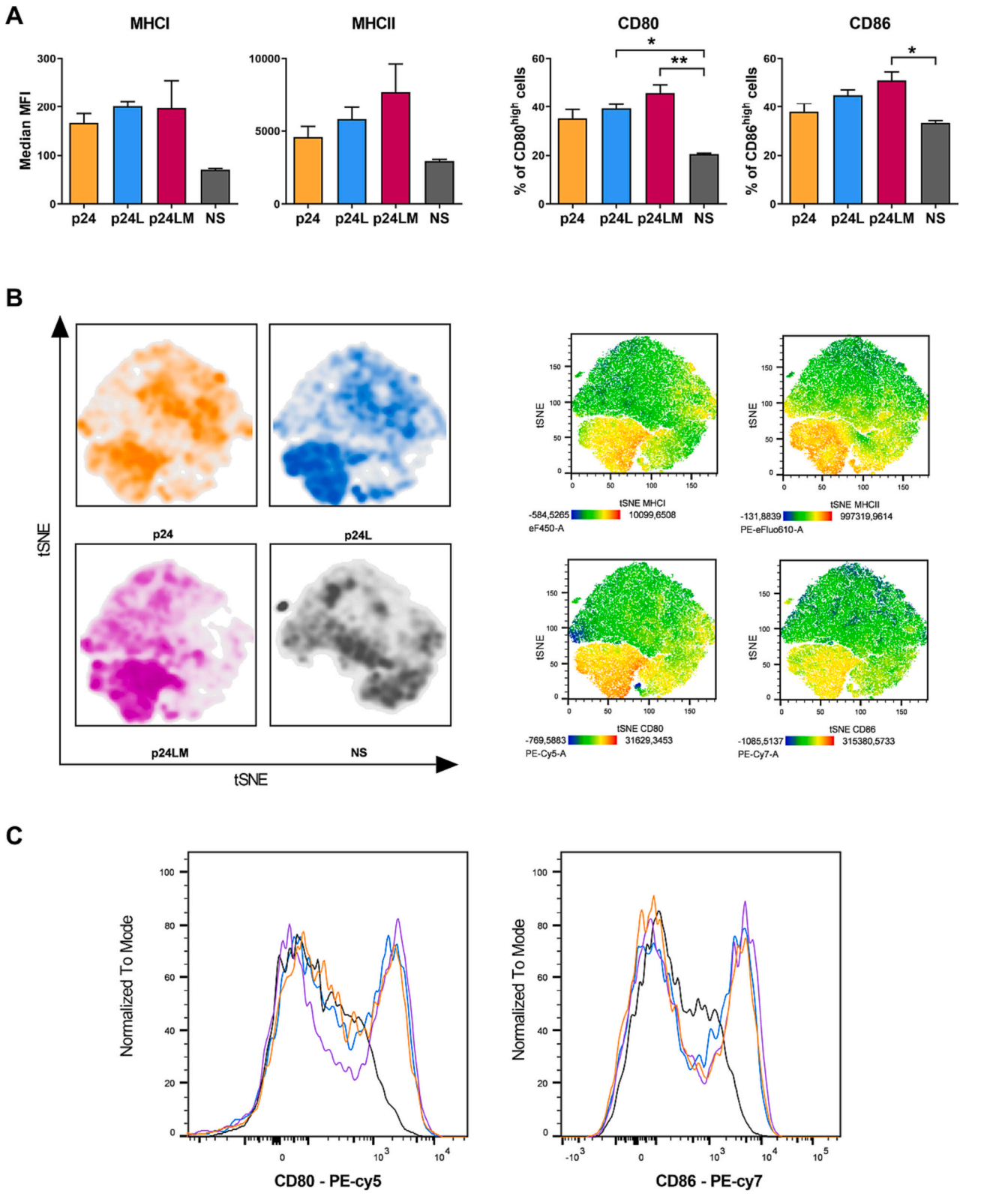

Fig. 4. BMDC activation.

Activation of BMDCs by p24 (orange), p24 coupled to liposome (p24L, blue) and p24 coupled to mannosylated liposome (p24LM, red) and not-pulsed cells (NS, grey). A) Differences of Median fluorescence intensity (MFI) in surface MHCI and MHCII marker expression and percentage of CD80 and CD86 positive cell populations of BMDCs pulsed by different antigenic constructs. Significant values were calculated by the ANOVA and Tukey post hoc test, where $*p < 0.05$, $**p < 0.01$. B) tSNE graphs of all proteo-liposomal constructs (p24, p24L, p24LM, NS) showing differences in marker expression on the left are followed by individual HeatMap projections of marker surface expression intensity on the right (FlowJo). After activation of DCs by particular construct, cell population expressing high MHCI, MHCII, CD80, and CD86 occur in the lower left quadrant of each graph. C) Histograms of normalized cell counts comparing CD80 and CD86 marker expression among groups.

Table 1
Activation of BMDC and MutuDC cells by p24, p24L, p24LM.

		p24	p24L	p24LM	NS
MutuDC	MHCI	49 ± 7	43 ± 1	43 ± 3	14 ± 3
	MHCII	4339 ± 220	7250 ± 913	6796 ± 1344	4982 ± 312
	CD40	1736 ± 236	1672 ± 408	1469 ± 366	768 ± 51
	CD80	346 ± 7	416 ± 42	447 ± 33	198 ± 8
	CD86	100 ± 4	138 ± 2	144 ± 28	49 ± 5
BMDC	MHCI	167 ± 28	201 ± 16	197 ± 82	71 ± 3
	MHCII	4588 ± 1043	5821 ± 1163	7702 ± 2734	2937 ± 186
	CD80	193 ± 59	220 ± 39	330,5 ± 153	130 ± 8
	CD86	179 ± 50	266 ± 64	514 ± 280	191 ± 11

Dendritic cell subsets differences. Differences of Median fluorescence intensity ± SD in surface MHCI, MHCII, CD80, CD86, and CD40 markers expression on DC subsets pulsed by different p24 constructs.

3. Discussion

3.1. Preparation and characterization of liposomal constructs

Yeasts, including *C. glabrata*, were shown to effectively induce the expression of the activation marker CD83, the co-stimulatory molecules CD80, CD86, CD54, CD58, and CD40, as well as the antigen-presenting molecules MHCI and MHCII on yeast-exposed DCs (Bazan, Walch-Ruckheim, Schmitt, & Breinig, 2018). Post-modification of liposomes by aminooxy coupling of mannan with biologically active molecules enables fast and easy binding of polysaccharides onto the surface of liposomes without changes in ability to interact with mannan receptors. In our previous studies we have demonstrated immunomodulatory activities of low molecular weight mannan from *C. glabrata* (Paulovicova et al., 2019). Coupling of this mannan onto liposomes via aminooxy condensation not only preserved, but even enhanced immunomodulatory activities of mannan as demonstrated on in vitro model of human dendritic cells (Bartheldyova et al., 2019). Therefore, based on previous results we have proposed liposomal mannan as suitable carrier platform for construction of recombinant vaccines. Because of preserving native orientation of mannan molecule on liposomal surface, aminooxy condensation-based "click chemistry" reaction was used for coupling. Preservation of native conformation was proved by immunogold staining as demonstrated at Fig. 2. The data are consistent with our previous study (Bartheldyova et al., 2019). Aminooxy coupling is highly chemo- and regio-selective strategy, hence it is also useful for the binding of polysaccharides-like mannans because only one reducing terminus

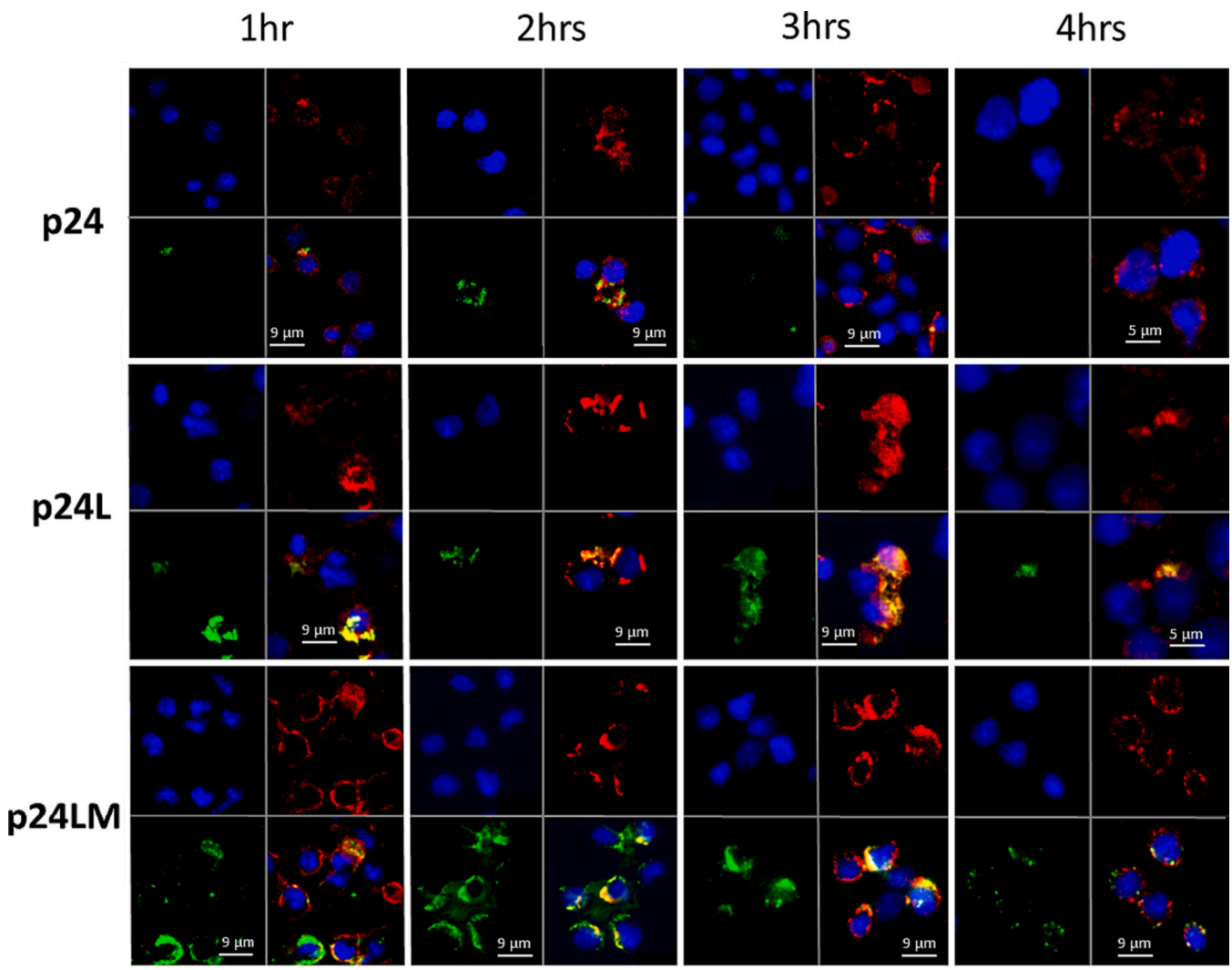

Fig. 5. Localization of the p24 antigen in MutuDC cells exposed p24, p24 bound to liposome, and p24 bound to mannosylated liposome.
MutuDC were exposed to individual p24 formulation for four different time points (1, 2, 3, and 4 h) and the antigen uptake was detected by confocal microscopy. Early endosome was detected by rabbit anti-EEA1 marker and anti-rabbit IgG-Cy3 (red), p24 was detected by anti-V5-FITC (green) and cell nuclei were stained by DAPI (blue). Upper row represents the p24 pulsed cells, the middle the p24L-pulsed cells and lower row represents cells pulsed with p24LM.

(hemiacetal) is present in each mannan molecule. From the point of view regarding the vaccine production it is important that the aminooxy coupling lacks any noxious by-products as only water is produced. Therefore, purification of final product mannan-modified liposomes is not necessary. Biocompatibility of vaccines is tightly linked with biodegradability of each component. The oxime bond formed by aminooxy coupling is thermodynamically unstable and undergoes hydrolysis under mildly acid conditions taking place in lysosomes. The same is true for non-covalent orthogonal binding of proteins with HisTag onto liposomes via metallochelating binding. Aminooxy based click chemistry represents simple methods used for preparation of various proteoliposomes (Lukac et al., 2011; Masek, Bartheldyova, Korvasova, et al., 2011; Masek, Bartheldyova, Turanek-Knotigova, et al., 2011) and can be easily used for coupling of His-tagged recombinant antigens onto mannan-modified liposomes. Because of simplicity of this conjugation method it is suitable also for preparation of vaccines in industrial scale under GMP conditions.

In the case of recombinant p24 we have reached dissociation constant $K_d \approx 10^{-8}$ (see table in Fig. 2), which means that the non-covalent metallochelating bond is stable, but can be cleaved in acidic milieu inside lysosomes and p24 antigen is thus ready to be processed and then presented via MHCII. Stability of metallochelating bond can be increased by one order of magnitude if doubling the HisTags in recombinant antigen is used as we proved in previous study (Petrokova et al., 2019). Suggested structure of mannan modified proteoliposomes as presented in Fig. 1A is in a good correlation with experimental data obtained from dynamic light scattering and electron microscopy (Figs. 1B and 2). Different stoichiometry coefficient for p24 binding onto plain and mannan-modified liposomes, respectively, means that there is a steric hindrance of p24 binding caused by mannan molecules (see table in Fig. 2).

Moreover, mannan modification of liposomes plays a crucial role in antigen escape from endosomes to cytosol (Bartheldyova et al., 2019; Gros & Amigorena, 2019; Moron, Rueda, Sedlik, & Leclerc, 2003; Ortega et al., 2015; Zachova et al., 2016). This step is critical and directly determines the antigen presentation pathway via MHCI or MHCII. Antigen remaining in endosomes fuses with lysosomes, the pH decreases rapidly and lysosomal proteases cleave the antigen in to peptides to be bound on MHCII molecules. By this canonical presentation pathway, $CD4^+$ T lymphocytes are stimulated by the antigen allowing subsequent B cell activation and neutralizing antibodies production. On the other hand, when antigen leaves the endosome, it could be then cleaved by proteasome, transported to endoplasmic reticulum, and bound on MHCI molecules. This alternative pathway called cross-presentation leads to $CD8^+$ T cell activation and differentiation into effector CTLs (Zachova et al., 2016), which are a part of effective defense mechanism against some viral infections and also tumors.

In general, mannosylated liposomes are recognized and internalized by DCs followed by stimulating signaling cascade, leading to expression of activation markers CD80, CD86, CD40, MHCI and MHCII (Bartheldyova et al., 2019). In a past few years many innovative methods of mannosylated liposomes preparation for recognition by mannose-specific lectin receptors of immune cells have been reported. These methods were used for treatment of respiratory intracellular parasitic infections, such as *Mycoplasma tuberculosis*, *Chlamydophila pneumonia*, *Listeria monocytogenes*, *Legionella pneumophila* and *Francisella tularensis* (Chono, Tanino, Seki, & Morimoto, 2008). *Leishmania donovani* (Mitra, Mandal, Chatterjee, & Das, 2005), and for potential vaccination against several pathogens, such as *Neisseria meningitis* (Arigita et al., 2003), *Leishmania major* (Shimizu et al., 2007), HIV (Sasaki et al., 1997; Toda et al., 1997) or several types of cancer (Lu, Kawakami, Yamashita, & Hashida, 2007; White, Rades, Kearns, Toth, & Hook, 2006). However, several limitations arise from the nature of this study. First, mice cells lines do not express the full set of human lectin receptors (Caminschi et al., 2006; Park et al., 2001; Takahara et al., 2004). Therefore, transferring our results to the human system will require further investigation using human cell lines or macrophages derived from peripheral blood monocytes. Also, we are aware that calcium and magnesium are playing key role in coordinating the binding between glycans and the carbohydrate recognition domains. But by using PBS and the proper controls we have seen that almost no false positive results were obtained.

In our study we evaluated the immunostimulatory effect of mannosylated liposomes containing p24 protein from HIV-1 virus on specific murine cell line MutuDC and BMDCs (Zachova et al., 2016). In MutuDC, p24L and p24LM significantly influences the MHCII expression in comparison to p24 alone, whereas expression of MHCI, CD80 and CD86 were significantly increased in all 3 formulations comparing to not pulsed cells. In BMDC expression of CD80 was increased only after the stimulation by p24L or p24LM and simultaneously the expression of CD86 was increased after the stimulation by p24LM and similar trend was observed for p24L. This is in agreement with previously published data which described that size of liposomes plays important role in stimulating of desired type of immune response (Badiee et al., 2012). Large liposomes generate lower production of proinflammatory cytokines as smallest vesicles (Henriksen-Lacey, Devitt, & Perrie, 2011) and stimulate Th1-immunity response with production of Active Ingredient γ (IFN- γ), whereas smaller vesicles efficiently generate Th2-immunity response with IL-5 production (Mann et al., 2009). In addition, antigens coupled to large vesicles are more efficiently presented on MHCII by APCs (Brewer, Pollock, Tetley, & Russell, 2004). Glycan-modified liposomes are better taken by DC or transported through Payer's patches M cells (Pukanud et al., 2009). High-mannose glycan-modified liposomes are taken by DCs expressing high-mannose receptor C-type lectin (DC- SIGN), Langerin or MR (CD206) and increase the antigen presentation by approximately 100-fold greater than unmodified liposomes (Raska & Novak, 2010; Unger et al., 2012). Modified liposomes also stimulate stronger Th1-immunity response with production of IL-2 and IFN-γ as unmodified liposomes (Gupta & Vyas, 2011; Hattori, Kawakami, Suzuki, Yamashita, & Hashida, 2004).

This idea is in agreement with previously published data, where mannosylated liposomes significantly increase association of liposome with macrophages (Kelly, Jefferies, & Cryan, 2011) but targeting additional receptors could enhance further the DC activation. In other studies, mannan coated cationic liposomes containing HIV-1 DNA activated cytotoxic T cells, IgA and other hypersensitivity immune responses (Coulibaly, Ezoulin, Dim, Molteni, & Youan, 2019) which is in agreement with DGS-NTA-liposomes with His-tagged Gag peptide that are capable to induce Th1 immune response against HIV Gag protein (Patel, O'Carra, Jones, Woodward, & Mumper, 2007). In DermaVir particles, small mannosylated cationic particles are in phase III of clinical testing [https://www.geneticimmunity.com/dermavir.html] where both $CD4^+$ and $CD8^+$ T cell responses were detected.

Immunological properties of p24 protein (p24), p24 protein coupled with liposome (p24L) and p24 protein coupled with mannosylated liposome (p24LM) were studied in two different murine cell subsets, the bone-marrow derived dendritic cells from BALB/c mouse representing the H2kD haplotype and in MutuDC immortalized cell line from C57BL/ 6 mouse representing the H2kB haplotype. Bone marrow derived den-dritic cells are widely used as a tool for antigen immunogenicity char-acterization. Nevertheless, different haplotype could show different properties to antigen processing, cutting into antigenic peptides and potential of T cell stimulating. MutuDC were described to be a perfect cross-priming cells being able to show the antigenic fragments not only on MHCII molecules, but particularly on MHCI molecules (Fuertes Marraco et al., 2012). This ability is very beneficial in anti-viral and anti- tumor vaccine design, where not only neutralizing antibodies but also cellular cytotoxic response is required.

p24-based vaccine represents an important component of future HIV-1 vaccine which should target both cellular immunity including cytotoxic T cells (primed after cross presentation of antigen reported here) as well as humoral immunity associated with neutralizing/binding anti-bodies on both systemic and mucosal compartment (Raska et al., 2008),

as the most effective way to prevent HIV-1 acquisition and spreading. Nevertheless, in contrast to cytotoxic T cell antigens, which could be produced in simple expression systems like prokaryotic, antigens inducing neutralizing/binding antibodies require posttranslational modification associated with much advanced expression system usage such as mammalian (Raska et al., 2014; Raska & Novak, 2010; Wei et al., 2020).

4. Conclusion

Here we describe preparation and characterization of vaccination nanoparticles based on surface-modified nanoliposomes using metallochelating reaction and click chemistry reaction. Orthogonal binding of both mannan by aminooxy coupling click chemistry and recombinant p24 derived antigen by metallochelating reaction onto liposomal surface was achieved. The whole technology based on "click-chemistry" is transferrable into industrial scale processes meeting GMP. Metallochelating nanoliposomes adjuvanted by low molecular weight mannan derived from *C. glabrata* can be used as platform for construction of various vaccines based on recombinant antigens if specific and intensive immune response is required. Synthetic oligomannans resembling structure of low molecular weight mannan are under development by us to bring us closer to a fully synthetic vaccine. In vitro experiments proved targeting of these liposome-based nanoparticles toward dendritic cells via MR and stimulation of dendritic cell to present antigen by both MHCI and MHCII pathways. These promising in vitro data paved the way for in vivo immunization experiments on mice to study the intensity and character of antibody and cellular immune response. This in vivo study will be published separately as complementary paper to this one.

5. Methods

5.1. Chemicals

All chemicals, unless concretely mentioned, were purchased from Sigma-Aldrich (St. Louis, MO, US). Tissue-culture media and media supplements were purchased from Thermo Fisher Scientific (Waltham, MA, US).

5.2. p24 protein expression and purification

cDNA encoding viral p24 from HIV-1 was a generous gift from Dr. Bernard Verrier (BioMérieux, Lyon, France). The sequence of p24 was cloned into pET101/D-TOPO expression vector coding also His and V5 tag epitope sequences. Recombinant p24 was expressed in *E. coli* BL21 (DE3) after induction with 1 mM Isopropyl β-D-1-thiogalactopyranoside once OD_{600} of the bacteria culture reached 0.6. Four hours after induction the cell culture was pelleted and recombinant p24 protein was isolated using Ni-NTA affinity chromatography (Zachova et al., 2009). Lipopolysaccharides coming from bacteria were eliminated from the purified p24 protein sample by Triton X-114 extraction (Krupka et al., 2015; Zachova et al., 2009). Final endotoxin level was determined to be lower than 2.5 EU/mg of protein using Limulus amaebocyte lysate gel-clot assay Pyrotell (Associated of Cape Cod, MA, USA). The 3D structure of p24 was predicted by Phyre2 Protein Fold Recognition Server (Creative Commons, CA, US).

5.3. Differential scanning calorimeter

Differential scanning calorimeter (DSC) (MicroCal-PEAQ DSC, Malvern, UK) was used for detection of phase transition of p24. Samples were at concentration 6×10^{-6} M, thermal stability was measured in the range 5–130 °C with scan rate 60 °C per hour with high feedback.

5.4. Multi-angle dynamic light scattering

The hydrodynamic diameters of examined nanoparticles were determined by dynamic light scattering instrument Zetasizer ULTRA (Malvern, UK) at 25 °C using cuvette ZEN2112 of 50 μl volume.

5.5. Preparation of metallochelation liposomes with attached p24 antigen

Metallochelation liposomes were prepared using the method based on hydration of a lipid film followed by extrusion through 0.1 μm polycarbonate filters with the hand operated device The HandExtruder (Genizer, CA, USA). The lipid composition was as follows: 7 % DGS-NTA-Ni (1,2-dioleoyl-sn-glycero-3-[(N-(5-amino-1-carboxypentyl)iminodiacetic acid)succinyl]nickel salt), 1 % N-oxy, 92 % EPC (Egg phosphatidyl choline). The solution of p24 in PBS (p24: DGS-NTA-Ni molar ratio of 1:10; 0.227 mg p24: 1 mg total lipid) was mixed with the prepared metallochelation liposomes. The mixture was stirred for 120 min.

5.6. Production of Candida glabrata cellular mannan and its orthogonal binding onto p24-liposomes by N-oxy ligation

Extraction and purification of cellular mannan was performed according to (Bartheldyova et al., 2019; Paulovicova et al., 2019). Briefly, yeast strain *C. glabrata* CCY 26-20-1 (Culture Collection of Yeast, Institute of Chemistry of Slovak Academy of Science, Center for Glycomics Bratislava, Slovakia) was grown on semi-synthetic medium for 4 days. Acido-stabile part of *C. glabrata* cellular mannan was extracted by autoclaving in 0.2 mol/l NaCl (140 °C, 700 kPa) for 90 min and purified using precipitation with Fehling's reagent (Peat & Rees, 1961).

The binding of mannan molecules onto p24 liposomes was performed as described in (Bartheldyova et al., 2019) with a slight difference. p24 proteoliposomes were used in the reaction instead of plain metallochelation liposomes. The total lipid to mannan ratio was 10:1 during the reaction.

5.7. Isothermal titration calorimetry (ITC)

Gradual addition of the liposomal solution (lipid concentration 0.1 mg/ml) from a syringe with a volume of 40 μl to the titrated protein solution (0.4 mg/ml) with a volume of 350 μl located in a cell was performed using MicroCal PEAQ calorimeter (Malvern, UK). Experiments were performed in 50 mM Tris buffer with 0.9 % NaCl, pH 7.4, without mixing and at temperature of 25 °C.

5.8. Electron microscopy methods

5.8.1. Contrasting proteoliposomes

The 10 ul of sample was put on grid (Formvar layered, 400 mesh, copper, Agar Scientific, UK) for 7 min. The seated liposomes were negatively stained with 2 % ammonium molybdate tetrahydrate for 2 min. The sample was observed and documented in transmission electron microscope Morgagni 268D TEM (Thermo Fisher Scientific, Eindhoven, Netherlands) working on 90 kV and equipped with a Veleta CCD camera (Olympus, Münster, Germany). The images were taken on 180,000× magnification. Amount of antibody and colloidal gold was chosen as small as possible to avoid protein precipitation.

5.9. Specific immunogold labeling of mannan on the manosylated p24 proteoliposomes

Labeling was performed as described earlier by Bartheldyova et al. (Bartheldyova et al., 2019; Masek, Bartheldyova, Korvasova, et al., 2011; Masek, Bartheldyova, Turanek-Knotigova, et al., 2011). Briefly, 4 μg of recombinant human mannose receptor CD206 (MMR, R&D Systems; Minneapolis, USA) was mixed with 3 mg of mannosylated liposomes (10 mg/ml PBS). The mixture was stirred at room temperature for

1 h. In the next step, 10 μg of mouse anti-HisTag monoclonal antibody (1 mg/ml, ThermoFisher Scientific, Waltham, USA) was added. Nominal size 20 nm Protein-A gold nanoparticles were diluted to the ratio 1:50 and then gold nanoparticles (Electron Microscopy Science, USA) and complete liposomal sample were mixed in the volume ratio 1:1. The mixture was incubated overnight at 4 °C.

The resulting suspension was covered with a Cu grid (300 Old Mesh, Agar Scientific, Austria) coated with Formvar film and carbon. The grid was removed from the suspension after 1 min, and the residual water was dried with a strip of lint-free filtration paper. The sample was stained with 2 % Ammonium molybdate and observed under transmission electron microscope Philips 208S Morgagni (FEI, Czech Republic) at 80 kV and magnification 18,000×.

5.10. Specific immunogold labelling of p24 and mannan using transmission electron microscopy

Specific immunogold labelling of p24 was performed as follows: p24 proteoliposomes were incubated with monoclonal anti-V5 antibody (1:2000) for 1 h at 37 °C. Nominal size 10 nm colloidal gold–protein A conjugate (1:20) (Electron Microscopy Science, USA) was added. After 12 h incubation, proteoliposomes were observed (Masek, Bartheldyova, Korvasova, et al., 2011; Masek, Bartheldyova, Turanek-Knotigova, et al., 2011).

5.11. Differentiation of bone marrow-derived dendritic cells from BALB/c mouse

Bone marrow-derived DCs (BMDC) were differentiated from monocytes in GM-CSF and IL-4 cytokine environment as was described previously (Krupka et al., 2015). Shortly, femurs and tibiae of BALB/c mouse were removed from mouse sacrificed under ketamine/xylazine an aesthesia. Bones were washed in PBS and remaining cells on the bone surfaces were fixed with 70 % ice-cold ethanol. Both epiphyses were excised and the bone marrow was flushed out using 20 ml syringe with needle filled with complete RPMI medium. Cell were pelleted 5 min at 250 ×*g* and remaining red blood cells were lysed with Red Blood Cell Lysis Buffer. Purified monocytes were seeded at final concentration 10^6/ml of complete RPMI medium containing 20 ng/ml GM-CSF, and 20 ng/ml IL-4. Cells were cultivated for 6 days in a humidified 5 % CO_2 incubator at 37 °C, when every second day 2/3 of cultivation media was replaced.

5.12. MutuDC cell line cultivation

MutuDC is an immortalized splenic DC line from C57BL/6 mouse described as a perfect presenting and cross-presenting tool for different studies (Fuertes Marraco et al., 2012). MutuDC cells are differentiated semi-adherent cells being cultivated in IMDM + Glutamax media containing 8 % FBS, 50 μM β-mercaptoethanol.

5.13. Activation of DC subsets by different proteo-liposomal constructs

Both BMDC and MutuDC were seeded into 24-well panel for flow cytometry analysis or into Multichamber slide (MutuDC after being treated by trypsin) at final concentration 10^6 cells per ml. Cells were pulsed in triplets for MutuDc and in doublets for BMDC by 12.5 μg p24 alone (p24), 12.5 μg p24 bound on liposome (p24L) and 12.5 μg p24 bound on liposome with mannan (p24LM) for 24 h for flow cytometry, or for 1, 2, 3, and 4 h for confocal microscopy analysis.

5.14. Confocal microscopy analysis

MutuDC were washed by PBS in Multichamber slide and all samples were fixed by 4 % paraformaldehyde for 10 min at RT and permeabilized by 0.1 % Triton X-100 in PBS for 10 min at RT. Non-specific bonds were blocked by 1 % FBS + 0.1 % Triton X100 in PBS for 30 min at RT. Samples were cultivated in solution of primary antibody contained rabbit anti-EEA1 (1:100) in 1 % FBS in PBS for 1 h at RT. After 3-times of PBS washing, secondary or conjugated antibody were added in dilution of goat anti-rabbit IgG-cy3 (1:1000) and mouse anti-V5-FITC (1:500) and incubated for 30 min at RT in the dark. Samples were washed 3-times by PBS, mounted with Vectashield mounting media containing DAPI (Vector, Burlingame, CA, USA). Samples were analyzed by confocal microscope Leica SP8 (Wetzlar, Germany) equipped with white laser. Excitation laser was set to 488 nm for FITC, and to 561 nm for Cy3. 405 nm UV laser was used for excitation of DAPI.

5.15. Flow cytometry analysis

24 h after pulsation BMDC with p24, p24L, or p24LM cells were washed by PBS, mutuDC were treated with trypsin and washed by PBS. 10^6 cells were stained with fluorochrome-conjugated antibodies – anti-CD11c-eFluor506, anti-MHCI(H2kD)-eFluor450, anti-MHCI(H2kB)-eFluor450, anti-MHCII-PE-eFluor610, anti-CD40-PE, anti-CD80-PE-cy7 and anti-CD86-PE-cy5 (eBioscience, MA, USA) for 30 min at RT in the dark. Cells were washed by PBS and analyzed on SONY SP6800 spectral analyser (SONY Biotechnologies, Japan).

Supplementary data to this article can be found online at https://doi.org/10.1016/j.carbpol.2024.121844.

Data analyses

All cytometry data were analyzed using SONY software (SONY Biotechnologies, Japan) and FlowJo 10.6.1 version software (Becton Dickinson, NJ, USA). Statistical data analyses were performed using GraphPad Prism 8 software (CA, USA).

Funding

The research was supported by the Ministry of Health, Czech Republic conceptual development of research organization grant MHCZ-DRO, FNOL, 00098892 (KZ, MR), by the Ministry of School, Youth, and Sport, Czech Republic grant CEREBIT CZ. 02.1.01/0.0/0.0/16_025/0007397 (MR, JT) and European Regional Development Fund Project ENOCH, CZ.02.1.01/0.0/0.0/16_019/0000868 (MR, JT), Palacky University grant IGA_LF_2023_010 (MR, MK). The support was also obtained from the internal project of NEXARS (JT, RH).

We acknowledged the access to the instruments supported by the project MPO REBIONVAC CZ.01.1.02/0.0/0.0/20_338/0023819 (JT) and the OPVVV PO1 project "FIT" CZ.02.1.01/0.0/0.0/15_003/0000495 (JT, MR).

CRediT authorship contribution statement

K. Zachová: Data curation, Writing – original draft. **E. Bartheldyová:** Data curation, Investigation, Writing – original draft. **F. Hubatka:** Data curation, Investigation. **M. Křupka:** Investigation. **N. Odehnalová:** Investigation. **P. Turánek Knötigová:** Investigation. **N. Vaškovicová:** Investigation. **K. Sloupenská:** Investigation. **R. Hromádka:** Resources. **E. Paulovičová:** Conceptualization, Resources, Validation. **R. Effenberg:** Conceptualization, Investigation. **M. Ledvina:** Conceptualization. **M. Raška:** Conceptualization, Funding acquisition, Supervision, Writing – original draft, Writing – review & editing. **J. Turánek:** Conceptualization, Data curation, Methodology, Supervision, Writing – review & editing.

Declaration of competing interest

The authors declare that they have no known competing financial interests or personal relationships that could have appeared to influence the work reported in this paper.

Data availability

All data generated or analyzed during this study are included in this published article and its Supplementary information files.

Acknowledgement

We thank to prof. Hans Acha-Orbea, Ph.D., Department of Biochemistry, University of Lausagne, Switzerland for the MutuDC cell line providing.

We acknowledged the technical assistance of Pharm.Dr. Josef Masek, Ph.D. with confocal microscopy.

References

Alshehri, A., Grabowska, A., & Stolnik, S. (2018). Pathways of cellular internalisation of liposomes delivered siRNA and effects on siRNA engagement with target mRNA and silencing in cancer cells. *Scientific Reports, 8*(1), 3748.

Arab, A., Behravan, J., Razazan, A., Gholizadeh, Z., Nikpoor, A. R., Barati, N., … Jaafari, M. R. (2018). A nano-liposome vaccine carrying E75, a HER-2/neu-derived peptide, exhibits significant antitumour activity in mice. *Journal of Drug Targeting, 26*(4), 365–372.

Arigita, C., Kersten, G. F., Hazendonk, T., Hennink, W. E., Crommelin, D. J., & Jiskoot, W. (2003). Restored functional immunogenicity of purified meningococcal PorA by incorporation into liposomes. *Vaccine, 21*(9–10), 950–960.

Badiee, A., Khamesipour, A., Samiei, A., Soroush, D., Shargh, V. H., Kheiri, M. T., … Jaafari, M. R. (2012). The role of liposome size on the type of immune response induced in BALB/c mice against leishmaniasis: rgp63 as a model antigen. *Experimental Parasitology, 132*(4), 403–409.

Bartheldyova, E., Turanek Knotigova, P., Zachova, K., Masek, J., Kulich, P., Effenberg, R., … Turanek, J. (2019). N-Oxy lipid-based click chemistry for orthogonal coupling of mannan onto nanoliposomes prepared by microfluidic mixing: Synthesis of lipids, characterisation of mannan-coated nanoliposomes and in vitro stimulation of dendritic cells. *Carbohydrate Polymers, 207*, 521–532.

Bazan, S. B., Walch-Ruckheim, B., Schmitt, M. J., & Breinig, F. (2018). Maturation and cytokine pattern of human dendritic cells in response to different yeasts. *Medical Microbiology and Immunology, 207*(1), 75–81.

Brewer, J. M., Pollock, K. G., Tetley, L., & Russell, D. G. (2004). Vesicle size influences the trafficking, processing, and presentation of antigens in lipid vesicles. *Journal of Immunology, 173*(10), 6143–6150.

Bulbake, U., Doppalapudi, S., Kommineni, N., & Khan, W. (2017). Liposomal formulations in clinical use: An updated review. *Pharmaceutics, 9*(2).

Caminschi, I., Corbett, A. J., Zahra, C., Lahoud, M., Lucas, K. M., Sofi, M., … Wright, M. D. (2006). Functional comparison of mouse CIRE/mouse DC-SIGN and human DC-SIGN. *International Immunology, 18*(5), 741–753.

Cawlfield, A., Genito, C. J., Beck, Z., Bergmann-Leitner, E. S., Bitzer, A. A., Soto, K., … Dutta, S. (2019). Safety, toxicity and immunogenicity of a malaria vaccine based on the circumsporozoite protein (FMP013) with the adjuvant army liposome formulation containing QS21 (ALFQ). *Vaccine, 37*(29), 3793–3803.

Chono, S., Tanino, T., Seki, T., & Morimoto, K. (2008). Efficient drug targeting to rat alveolar macrophages by pulmonary administration of Active Ingredient incorporated into mannosylated liposomes for treatment of respiratory intracellular parasitic infections. *Journal of Controlled Release, 127*(1), 50–58.

Coulibaly, F. S., Ezoulin, M. J. M., Dim, D. C., Molteni, A., & Youan, B. C. (2019). Preclinical safety evaluation of HIV-1 gp120 responsive microbicide delivery system in C57BL/6 female mice. *Molecular Pharmaceutics, 16*(2), 595–606.

De Serrano, L. O., & Burkhart, D. J. (2017). Liposomal vaccine formulations as prophylactic agents: Design considerations for modern vaccines. *Journal of Nanobiotechnology, 15*(1), 83.

Effenberg, R., Turanek Knotigova, P., Zyka, D., Celechovska, H., Masek, J., Bartheldyova, E., … Turanek, J. (2017). Nonpyrogenic molecular adjuvants based on norAbu-muramyldipeptide and norAbu-glucosaminyl muramyldipeptide: Synthesis, molecular mechanisms of action, and biological activities in vitro and in vivo. *Journal of Medicinal Chemistry, 60*(18), 7745–7763.

Fuertes Marraco, S. A., Grosjean, F., Duval, A., Rosa, M., Lavanchy, C., Ashok, D., … Acha-Orbea, H. (2012). Novel murine dendritic cell lines: A powerful auxiliary tool for dendritic cell research. *Frontiers in Immunology, 3*, 331.

Gros, M., & Amigorena, S. (2019). Regulation of antigen export to the cytosol during cross-presentation. *Frontiers in Immunology, 10*, 41.

Gupta, P. N., & Vyas, S. P. (2011). Investigation of lectinized liposomes as M-cell targeted carrier-adjuvant for mucosal immunization. *Colloids and Surfaces. B, Biointerfaces, 82*(1), 118–125.

Hattori, Y., Kawakami, S., Suzuki, S., Yamashita, F., & Hashida, M. (2004). Enhancement of immune responses by DNA vaccination through targeted gene delivery using mannosylated cationic liposome formulations following intravenous administration in mice. *Biochemical and Biophysical Research Communications, 317*(4), 992–999.

Henriksen-Lacey, M., Devitt, A., & Perrie, Y. (2011). The vesicle size of DDA:TDB liposomal adjuvants plays a role in the cell-mediated immune response but has no significant effect on antibody production. *Journal of Controlled Release, 154*(2), 131–137.

Kanamala, M., Palmer, B. D., Ghandehari, H., Wilson, W. R., & Wu, Z. (2018). PEG-benzaldehyde-Hydrazone-lipid based PEG-sheddable pH-sensitive liposomes: Abilities for endosomal escape and long circulation. *Pharmaceutical Research, 35*(8), 154.

Kelly, C., Jefferies, C., & Cryan, S. A. (2011). Targeted liposomal drug delivery to monocytes and macrophages. *Journal of Drug Delivery, 2011*, Article 727241.

Knotigova, P. T., Zyka, D., Masek, J., Kovalova, A., Krupka, M., Bartheldyova, E., … Turanek, J. (2015). Molecular adjuvants based on nonpyrogenic lipophilic derivatives of norAbuMDP/GMDP formulated in nanoliposomes: Stimulation of innate and adaptive immunity. *Pharmaceutical Research, 32*(4), 1186–1199.

Koudelka, S., Mikulik, R., Masek, J., Raska, M., Turanek Knotigova, P., Miller, A. D., & Turanek, J. (2016). Liposomal nanocarriers for plasminogen activators. *Journal of Controlled Release, 227*, 45–57.

Krupka, M., Masek, J., Barkocziova, L., Turanek Knotigova, P., Kulich, P., Plockova, J., … Raska, M. (2016). The position of his-tag in recombinant OspC and application of various adjuvants affects the intensity and quality of specific antibody response after immunization of experimental mice. *PLoS One, 11*(2), Article e0148497.

Krupka, M., Masek, J., Bartheldyova, E., Turanek Knotigova, P., Plockova, J., Korvasova, Z., … Turanek, J. (2012). Enhancement of immune response towards non-lipidized Borrelia burgdorferi recombinant OspC antigen by binding onto the surface of metallochelating nanoliposomes with entrapped lipophilic derivatives of norAbuMDP. *Journal of Controlled Release, 160*(2), 374–381.

Krupka, M., Zachova, K., Cahlikova, R., Vrbkova, J., Novak, Z., Sebela, M., … Raska, M. (2015). Endotoxin-minimized HIV-1 p24 fused to murine hsp70 activates dendritic cells, facilitates endocytosis and p24-specific Th1 response in mice. *Immunology Letters, 166*(1), 36–44.

Kuai, R., Sun, X., Yuan, W., Xu, Y., Schwendeman, A., & Moon, J. J. (2018). Subcutaneous nanodisc vaccination with neoantigens for combination cancer immunotherapy. *Bioconjugate Chemistry, 29*(3), 771–775.

Lu, Y., Kawakami, S., Yamashita, F., & Hashida, M. (2007). Development of an antigen-presenting cell-targeted DNA vaccine against melanoma by mannosylated liposomes. *Biomaterials, 28*(21), 3255–3262.

Lukac, R., Kauerova, Z., Masek, J., Bartheldyova, E., Kulich, P., Koudelka, S., … Turanek, J. (2011). Preparation of metallochelating microbubbles and study on their site-specific interaction with rGFP-HisTag as a model protein. *Langmuir, 27*(8), 4829–4837.

Mann, J. F., Shakir, E., Carter, K. C., Mullen, A. B., Alexander, J., & Ferro, V. A. (2009). Lipid vesicle size of an oral influenza vaccine delivery vehicle influences the Th1/Th2 bias in the immune response and protection against infection. *Vaccine, 27*(27), 3643–3649.

Martin, C. A., Carsons, S. E., Kowalewski, R., Bernstein, D., Valentino, M., & Santiago-Schwarz, F. (2003). Aberrant extracellular and dendritic cell (DC) surface expression of heat shock protein (hsp)70 in the rheumatoid joint: Possible mechanisms of hsp/DC-mediated cross-priming. *Journal of Immunology, 171*(11), 5736–5742.

Masek, J., Bartheldyova, E., Korvasova, Z., Skrabalova, M., Koudelka, S., Kulich, P., … Turanek, J. (2011). Immobilization of histidine-tagged proteins on monodisperse metallochelation liposomes: Preparation and study of their structure. *Analytical Biochemistry, 408*(1), 95–104.

Masek, J., Bartheldyova, E., Turanek-Knotigova, P., Skrabalova, M., Korvasova, Z., Plockova, J., … Turanek, J. (2011). Metallochelating liposomes with associated lipophilised norAbuMDP as biocompatible platform for construction of vaccines with recombinant His-tagged antigens: Preparation, structural study and immune response towards rHsp90. *Journal of Controlled Release, 151*(2), 193–201.

Mitra, M., Mandal, A. K., Chatterjee, T. K., & Das, N. (2005). Targeting of mannosylated liposome incorporated benzyl derivative of Penicillium nigricans derived compound MT81 to reticuloendothelial systems for the treatment of visceral leishmaniasis. *Journal of Drug Targeting, 13*(5), 285–293.

Moron, V. G., Rueda, P., Sedlik, C., & Leclerc, C. (2003). In vivo, dendritic cells can cross-present virus-like particles using an endosome-to-cytosol pathway. *Journal of Immunology, 171*(5), 2242–2250.

Nagy, N. A., Castenmiller, C., Vigario, F. L., Sparrius, R., van Capel, T. M. M., de Haas, A. M., … de Jong, E. C. (2022). Uptake kinetics of liposomal formulations of differing charge influences development of in vivo dendritic cell immunotherapy. *Journal of Pharmaceutical Sciences, 111*(4), 1081–1091.

Nam, H. J., Hong, S. J., Lee, A., Kim, J., Lee, S., Casper, C., … Shin, E. C. (2022). An adjuvanted zoster vaccine elicits potent cellular immune responses in mice without QS21. *NPJ Vaccines, 7*(1), 45.

Ortega, R. A., Barham, W. J., Kumar, B., Tikhomirov, O., McFadden, I. D., Yull, F. E., & Giorgio, T. D. (2015). Biocompatible mannosylated endosomal-escape nanoparticles enhance selective delivery of short nucleotide sequences to tumor associated macrophages. *Nanoscale, 7*(2), 500–510.

Park, C. G., Takahara, K., Umemoto, E., Yashima, Y., Matsubara, K., Matsuda, Y., … Steinman, R. M. (2001). Five mouse homologues of the human dendritic cell C-type lectin, DC-SIGN. *International Immunology, 13*(10), 1283–1290.

Patel, J. D., O'Carra, R., Jones, J., Woodward, J. G., & Mumper, R. J. (2007). Preparation and characterization of nickel nanoparticles for binding to his-tag proteins and antigens. *Pharmaceutical Research, 24*(2), 343–352.

Paulovicova, L., Paulovicova, E., Farkas, P., Cizova, A., Bystricky, P., Jancinova, V., … Hrubisko, M. (2019). Bioimmunological activities of Candida glabrata cellular mannan. *FEMS Yeast Research, 19*(2).

Peat, S., & Rees, D. A. (1961). Carbohydrase and sulphatase activities of Porphyra umbilicalis. *The Biochemical Journal, 79*, 7–12.

Petrokova, H., Masek, J., Kuchar, M., Viteckova Wunschova, A., Stikarova, J., Bartheldyova, E., … Turanek, J. (2019). Targeting human thrombus by liposomes modified with anti-fibrin protein binders. *Pharmaceutics, 11*(12).

Pukanud, P., Peungvicha, P., & Sarisuta, N. (2009). Development of mannosylated liposomes for bioadhesive oral drug delivery via M cells of Peyer's patches. *Drug Delivery, 16*(5), 289–294.

Qu, W., Li, N., Yu, R., Zuo, W., Fu, T., Fei, W., … Yang, J. (2018). Cationic DDA/TDB liposome as a mucosal vaccine adjuvant for uptake by dendritic cells in vitro induces potent humoural immunity. *Artificial Cells, Nanomedicine, and Biotechnology, 46* (sup1), 852–860.

Raska, M., Czernekova, L., Moldoveanu, Z., Zachova, K., Elliott, M. C., Novak, Z., … Novak, J. (2014). Differential glycosylation of envelope gp120 is associated with differential recognition of HIV-1 by virus-specific antibodies and cell infection. *AIDS Research and Therapy, 11*, 23.

Raska, M., Moldoveanu, Z., Novak, J., Hel, Z., Novak, L., Bozja, J., … Mestecky, J. (2008). Delivery of DNA HIV-1 vaccine to the liver induces high and long-lasting humoral immune responses. *Vaccine, 26*(12), 1541–1551.

Raska, M., & Novak, J. (2010). Involvement of envelope-glycoprotein glycans in HIV-1 biology and infection. *Archivum Immunologiae et Therapiae Experimentalis (Warsz), 58* (3), 191–208.

Rayamajhi, S., Marchitto, J., Nguyen, T. D. T., Marasini, R., Celia, C., & Aryal, S. (2020). pH-responsive cationic liposome for endosomal escape mediated drug delivery. *Colloids and Surfaces. B, Biointerfaces, 188*, Article 110804.

Sasaki, S., Fukushima, J., Arai, H., Kusakabe, K. I., Hamajima, K., Ishii, N., … Okuda, K. (1997). Human immunodeficiency virus type-1-specific immune responses induced by DNA vaccination are greatly enhanced by mannan-coated diC14-amidine. *European Journal of Immunology, 27*(12), 3121–3129.

Shearer, L. J., & Petersen, N. O. (2019). Distribution and co-localization of endosome markers in cells. *Heliyon, 5*(9), Article e02375.

Shimizu, Y., Takagi, H., Nakayama, T., Yamakami, K., Tadakuma, T., Yokoyama, N., & Kojima, N. (2007). Intraperitoneal immunization with oligomannose-coated liposome-entrapped soluble leishmanial antigen induces antigen-specific T-helper type immune response in BALB/c mice through uptake by peritoneal macrophages. *Parasite Immunology, 29*(5), 229–239.

Stocki, P., Wang, X. N., & Dickinson, A. M. (2012). Inducible heat shock protein 70 reduces T cell responses and stimulatory capacity of monocyte-derived dendritic cells. *The Journal of Biological Chemistry, 287*(15), 12387–12394.

Takahara, K., Yashima, Y., Omatsu, Y., Yoshida, H., Kimura, Y., Kang, Y. S., … Inaba, K. (2004). Functional comparison of the mouse DC-SIGN, SIGNR1, SIGNR3 and Langerin, C-type lectins. *International Immunology, 16*(6), 819–829.

Toda, S., Ishii, N., Okada, E., Kusakabe, K. I., Arai, H., Hamajima, K., … Okuda, K. (1997). HIV-1-specific cell-mediated immune responses induced by DNA vaccination were enhanced by mannan-coated liposomes and inhibited by anti-Active Ingredient- gamma antibody. *Immunology, 92*(1), 111–117.

Unger, W. W., van Beelen, A. J., Bruijns, S. C., Joshi, M., Fehres, C. M., van Bloois, L., … van Kooyk, Y. (2012). Glycan-modified liposomes boost CD4+ and CD8+ T-cell responses by targeting DC-SIGN on dendritic cells. *Journal of Controlled Release, 160* (1), 88–95.

Vo, M. C., Nguyen-Pham, T. N., Lee, H. J., Jung, S. H., Choi, N. R., Hoang, M. D., … Lee, J. J. (2017). Chaetocin enhances dendritic cell function via the induction of heat shock protein and cancer testis antigens in myeloma cells. *Oncotarget, 8*(28), 46047–46056.

Wei, Q., Hargett, A. A., Knoppova, B., Duverger, A., Rawi, R., Shen, C. H., … Novak, J. (2020). Glycan positioning impacts HIV-1 Env glycan-shield density, function, and recognition by antibodies. *iScience, 23*(11), Article 101711.

White, K., Rades, T., Kearns, P., Toth, I., & Hook, S. (2006). Immunogenicity of liposomes containing lipid core peptides and the adjuvant Quil A. *Pharmaceutical Research, 23* (7), 1473–1481.

Zachova, K., Krupka, M., Chamrad, I., Belakova, J., Horynova, M., Weigl, E., … Raska, M. (2009). Novel modification of growth medium enables efficient E. coli expression and simple purification of an endotoxin-free recombinant murine hsp70 protein. *Journal of Microbiology and Biotechnology, 19*(7), 727–733.

Zachova, K., Krupka, M., & Raska, M. (2016). Antigen cross-presentation and heat shock protein-based vaccines. *Archivum Immunologiae et Therapiae Experimentalis (Warsz), 64*(1), 1–18.